

The Flash–Quench Technique in Protein–DNA Electron Transfer: Reduction of the Guanine Radical by Ferrocycytochrome *c*

Eric D. A. Stemp[†] and Jacqueline K. Barton*

Division of Chemistry and Chemical Engineering, California Institute of Technology, Pasadena, California 91125

Received January 20, 2000

Electron transfer from a protein to oxidatively damaged DNA, specifically from ferrocycytochrome *c* to the guanine radical, was examined using the flash–quench technique. Ru(phen)₂dppz²⁺ (dppz = dipyrrophenazine) was employed as the photosensitive intercalator, and ferricytochrome *c* (Fe³⁺ cyt *c*), as the oxidative quencher. Using transient absorption and time-resolved luminescence spectroscopies, we examined the electron-transfer reactions following photoexcitation of the ruthenium complex in the presence of poly(dA–dT) or poly(dG–dC). The luminescence-quenching titrations of excited Ru(phen)₂dppz²⁺ by Fe³⁺ cyt *c* are nearly identical for the two DNA polymers. However, the spectral characteristics of the long-lived transient produced by the quenching depend strongly upon the DNA. For poly(dA–dT), the transient has a spectrum consistent with formation of a [Ru(phen)₂dppz³⁺, Fe²⁺ cyt *c*] intermediate, indicating that the system regenerates itself via electron transfer from the protein to the Ru(III) metallointercalator for this polymer. For poly(dG–dC), however, the transient has the characteristics expected for an intermediate of Fe²⁺ cyt *c* and the neutral guanine radical. The characteristics of the transient formed with the GC polymer are consistent with rapid oxidation of guanine by the Ru(III) complex, followed by slow electron transfer from Fe²⁺ cyt *c* to the guanine radical. These experiments show that electron holes on DNA can be repaired by protein and demonstrate how the flash–quench technique can be used generally in studying electron transfer from proteins to guanine radicals in duplex DNA.

Introduction

Electron-transfer reactions of DNA have generated tremendous interest because oxidative damage to DNA has been implicated as a major factor in aging and molecular disease.¹ The heterocyclic bases are the most reactive moieties of the nucleic acids, and guanine (G) is the most easily oxidizable base and the ultimate resting site for electron holes in DNA.² Determining the fates of oxidized guanine is thus a fundamental component of understanding oxidative damage in a cell. While it is well-established that 8-oxoguanine is a major product of guanine oxidation, this lesion is not the only possible fate for oxidized guanine.³ In particular, the guanine radical could also be repaired by electron transfer with redox-active species such as proteins, as we describe here.

The flash–quench methodology, first developed for the study of electron transfer in proteins,⁴ offers an excellent platform for studying electron-transfer reactions involving guanine radicals. Other approaches such as pulse radiolysis⁵ or photoionization⁶ can lead to multiple damage sites on the DNA. In contrast, the flash–quench method allows for the selective oxidation of the guanine base in double-stranded DNA, using

only an intercalator, quencher, and visible light. In the flash–quench technique, visible light is used to excite a DNA-bound intercalator, which, upon electron transfer to an oxidative quencher, can oxidize G. Using ethidium as the intercalator and methyl viologen as the quencher, Dunn et al. showed that guanine-specific damage occurs in plasmids and restriction fragments.⁷ Employing Ru(phen)₂dppz²⁺ as the intercalator and Ru(NH₃)₆³⁺ as the quencher, we generated the guanine radical in double-stranded DNA⁸ and showed its spectrum to be similar to that of the neutral radical⁹ by transient absorption spectroscopy. In this study with poly(dG–dC), the formation of guanine radical was found to be concomitant with formation of the Ru(III) intercalator, occurring in ~50 ns.⁸ Moreover, the radical was found to be mobile; damage has been observed up to 198 Å from the site of oxidation.¹⁰

Given that the electron-transfer reactions of proteins¹¹ and of DNA¹² are both areas of intense research, there have been surprisingly few studies addressing electron transfers between

* To whom correspondence should be addressed.

[†] Present address: Mount St. Mary's College, Los Angeles, CA 90049.

- (1) (a) Kelly, S. O.; Barton, J. K. *Met. Ions Biol. Syst.* **1999**, *36*, 211. (b) Wiseman, H.; Halliwell, B. *Biochem. J.* **1996**, *313*, 17.
- (2) (a) Faraggi, M.; Broitman, F.; Trent, J. B.; Klapper, M. H. *J. Phys. Chem.* **1996**, *100*, 14751. (b) Steenken, S. *Free Radical Res. Commun.* **1992**, *16*, 349. (c) Steenken, S.; Jovanovic, S. *J. Am. Chem. Soc.* **1997**, *119*, 617. (d) Jovanovic, S. V.; Simic, M. G. *J. Phys. Chem.* **1986**, *90*, 974.
- (3) Burrows, C. J.; Muller, J. G. *Chem. Rev.* **1998**, *98*, 1109.
- (4) Chang, I. J.; Gray, H. B.; Winkler, J. R. *J. Am. Chem. Soc.* **1991**, *113*, 7056.

- (5) (a) Symons, M. C. R. *Free Radical Biol. Med.* **1997**, *22*, 1271. (b) Symons, M. C. R. *J. Chem. Soc., Faraday Trans.* **1987**, *83*, 1. (c) O'Neill, P.; Fielden, E. M. *Adv. Radiat. Biol.* **1993**, *17*, 53. (d) Vonsonntag, C.; Schuchmann, H. P. *Oxygen Radicals Biol. Syst.* **1994**, *233*, 3.
- (6) (a) Melvin, T.; Botchway, S.; Parker, A. W.; O'Neill, P. O. *J. Chem. Soc., Commun.* **1995**, 653. (b) Melvin, T.; Plumb, M. A.; Botchway, S.; Parker, A. W.; O'Neill, P. O.; Parker, A. W. *Photochem. Photobiol.* **1995**, *61*, 653.
- (7) Dunn, D. A.; Lin, V. H.; Kochevar, I. E. *Biochemistry* **1992**, *31*, 11620.
- (8) Stemp, E. D. A.; Arkin, M. R.; Barton, J. K. *J. Am. Chem. Soc.* **1997**, *119*, 2921.
- (9) Candeias, L. P.; Steenken, S. *J. Am. Chem. Soc.* **1989**, *111*, 1094–1099.
- (10) (a) Arkin, M. R.; Stemp, E. D. A.; Pulver, S. C.; Barton, J. K. *Chem. Biol.* **1997**, *4*, 389. (b) Núñez, M. E.; Hall, D. B.; Barton, J. K. *Chem. Biol.* **1999**, *6*, 85.

proteins and DNA. Perhaps the best example is the enzyme photolyase, which, upon absorption of visible light, repairs pyrimidine–pyrimidine dimers by injection of an electron into the cyclobutane adduct.¹³ Other researchers have shown that oxidized guanosine can be reduced by tyrosine and tryptophan in solution,¹⁴ suggesting that these aromatic residues could repair electron holes in DNA; indeed, electron holes generated by γ radiation in the guanine bases of chromatin appear to be transferred to the nearby histones.¹⁵ Moreover, we recently showed that guanine radicals in duplex DNA readily oxidize tryptophan or tyrosine in the intercalating tripeptides, Lys-Trp-Lys or Lys-Tyr-Lys.¹⁶ Clearly, electron transfer between proteins and DNA is relevant to the repair of DNA damage, and there will surely be more examples of such reactions.

The ubiquitous electron carrier cytochrome *c* (cyt *c*) is an excellent model protein for illustrating protein-to-DNA electron transfer. Cytochrome *c* is a basic protein with a ring of lysines surrounding its heme,¹⁷ and so the protein may associate with DNA electrostatically, probably with a redox-active group near the DNA surface. Cytochrome *c* plays an important role in apoptosis,¹⁸ activating proteolytic enzymes called caspases once released from mitochondria into the cytosol. Under normal conditions, interactions between cytochrome *c* and DNA are unlikely, because the mitochondrial DNA is situated in the matrix while the cytochrome resides in the intermembrane space. However, given that its basic face is rich in lysines, and that some histones are also lysine-rich,¹⁹ cyt *c* could serve as a model for DNA–histone interactions. Cyt *c* also has a strongly colored heme chromophore²⁰ ideal for monitoring electron-transfer kinetics.

Here, we employ the flash–quench technique to study electron transfer from a protein to DNA, specifically from Fe²⁺ cyt *c* to the guanine radical. Using time-resolved luminescence spectroscopy, we show that Fe³⁺ cyt *c* quenches photoexcited Ru(phen)₂dppz²⁺ in the presence of DNA. Using transient absorption spectroscopy, we also monitor the products of the redox quenching and find that the composition of these species depends on the sequence composition of the DNA used. With poly(dA–dT), the system returns to the ground state via a recombination reaction between Fe²⁺ cyt *c* and Ru(phen)₂dppz³⁺. In contrast, with poly(dG–dC), Ru(phen)₂dppz³⁺ rapidly produces the guanine radical and the observed electron transfer is from ferrocycytochrome *c* to the guanine radical. This electron-transfer reaction illustrates how redox-active proteins could play a role in the repair of oxidative damage in vivo.

Experimental Section

Materials. Hexaammineruthenium(III) chloride, potassium antimonyl tartrate, monobasic potassium phosphate, and potassium ferricyanide were obtained from Aldrich and used as received. Tris base and SP Sephadex C-25 and Sephadex G-25 resins were purchased from Sigma. Ru(phen)₂dppzCl₂ was prepared as described previously²¹ and purified by reversed-phase HPLC to remove trace impurities. The pure racemic complex was resolved into its Δ and Λ enantiomers by chromatography on an ion-exchange resin (SP Sephadex C-25) utilizing a chiral eluent (potassium antimonyl tartrate), as described elsewhere;²² all experiments were performed with the Δ enantiomer. Poly(dG–dC) and poly(dA–dT) were purchased from Pharmacia and were exchanged into a buffer of 5 mM Tris, 5 mM NaCl (pH 8) via ultrafiltration (Centricon 100, Amicon) prior to use. Horse heart cytochrome *c* (Sigma), purified to homogeneity by ion-exchange chromatography,²³ was a gift from Dr. Jason Telford. Complete conversion of the cytochrome to the oxidized form was accomplished by treatment with Fe(CN)₆Cl₃, followed by purification on Sephadex G-25 before use. Stock solutions were prepared by utilizing the extinction coefficients $\epsilon_{276} = 0.460 \text{ mM}^{-1} \text{ cm}^{-1}$ for Ru(NH₃)₆³⁺,²⁴ $\epsilon_{440} = 21.0 \text{ mM}^{-1} \text{ cm}^{-1}$ for Ru(phen)₂dppz²⁺,²⁵ $\epsilon_{410} = 106 \text{ mM}^{-1} \text{ cm}^{-1}$ for Fe³⁺ cytochrome *c*,²⁰ $\epsilon_{262} = 6.60 \text{ mM}^{-1} \text{ cm}^{-1}$ for poly(dA–dT), and $\epsilon_{254} = 8.40 \text{ mM}^{-1} \text{ cm}^{-1}$ for poly(dG–dC), as given by the manufacturer; concentrations of DNA are given in nucleotides (nuc).

Spectroscopic Measurements. Time-resolved emission and absorption experiments with cytochrome *c* were carried out in a low ionic strength buffer of 5 mM Tris, 5 mM NaCl (pH 8) to facilitate attraction of the cationic protein to the anionic DNA. In titration experiments, small aliquots of a concentrated protein solution were added to samples containing the intercalator and DNA. Time-resolved luminescence and absorption measurements utilized the 480 nm output (1–2 mJ/pulse, Coumarin 480) of an excimer-pumped dye laser or the 532 nm output (5–10 mJ/pulse) of an Nd:YAG laser, as described elsewhere.²⁶ Emission of the ruthenium lumiphore was monitored at 610 nm. Emission intensities were obtained by integrating under the luminescence decay curve and were corrected for cytochrome absorption at the excitation wavelength. Luminescence lifetimes were obtained by fitting the decay curves using in-house software. Stern–Volmer plots were used to obtain bimolecular quenching constants (k_q), according to eqs 1 and 2, where I_0 is the emission intensity in the absence of quencher (Q), I is the emission intensity at quencher concentration [Q],

- (11) (a) Langen, R.; Chang, I.-J.; Germanas, J. P.; Richards, J. H.; Winkler, J. R.; Gray, H. B. *Science* **1995**, *268*, 1733. (b) Farver, O.; Pecht, I. *J. Am. Chem. Soc.* **1992**, *114*, 5764. (c) Isied, S. S. *Adv. Chem. Ser.* **1997**, *253*, 331. (d) Mutz, M. W.; McLendon, G. L.; Wishart, J. F.; Gaillard, E. R.; Corin, A. F. *Proc. Natl. Acad. Sci. U.S.A.* **1996**, *93*, 9521. (e) Zhou, J. S.; Nocek, J. M.; Devan, M. L.; Hoffman, B. M. *Science* **1995**, *269*, 204. (f) Moser, C. C.; Keske, J. M.; Warncke, K.; Farid, R. S.; Dutton, P. L. *Nature* **1992**, *355*, 796. (g) Conrad, D. W.; Zhang, H.; Stewart, D. E.; Scott, R. A. *J. Am. Chem. Soc.* **1992**, *114*, 9909. (h) Beratan, D. N.; Onuchic, J. N.; Winkler, J. R.; Gray, H. B. *Science* **1992**, *258*, 1740. (i) Wuttke, D. S.; Bjerrum, M. J.; Winkler, J. R.; Gray, H. B. *Science* **1992**, *256*, 1007.
- (12) (a) Kelley, S. O.; Barton, J. K. *Science* **1999**, *283*, 375. (b) Wan, C.; Fiebig, T.; Kelley, S. O.; Treadway, C. R.; Barton, J. K.; Zewail, A. H. *Proc. Natl. Acad. Sci. U.S.A.* **1999**, *96*, 6014. (c) Meggers, E.; Michel-Beyerle, M. E.; Giese, B. *J. Am. Chem. Soc.* **1998**, *120*, 12950. (d) Fukui, K.; Tanaka, K. *Angew. Chem., Int. Ed. Engl.* **1998**, *37*, 158. (e) Gasper, S. M.; Schuster, G. B. *J. Am. Chem. Soc.* **1997**, *119*, 12762. (f) Lewis, F. D.; Wu, T.; Zhang, Y.; Letsinger, R. L.; Greenfield, S. R.; Wasielewski, M. R. *Science* **1997**, *277*, 673. (g) Meade, T. J.; Kayyem, J. F. *Angew. Chem., Int. Ed. Engl.* **1995**, *34*, 351. (h) Murphy, C. J.; Arkin, M. R.; Jenkins, Y. J.; Ghatlia, N. D.; Bossman, S. H.; Turro, N. J.; Barton, J. K. *Science* **1993**, *262*, 1025. (i) Brun, A. M.; Harriman, A. *J. Am. Chem. Soc.* **1992**, *114*, 3656. (j) Kelley, S. O.; Jackson, N. M.; Hill, M. G.; Barton, J. K. *Angew. Chem., Int. Ed. Engl.* **1999**, *38*, 941.
- (13) (a) Langenbacher, T.; Zhao, X. D.; Bieser, G.; Heelis, P. F.; Sancar, A.; Michel-Beyerle, M. E. *J. Am. Chem. Soc.* **1997**, *119*, 10532. (b) Heelis, P. F.; Hartman, R. F.; Rose, S. D. *Chem. Soc. Rev.* **1995**, *24*, 289. (c) Begley, T. P. *Acc. Chem. Res.* **1994**, *27*, 394.
- (14) Jovanovic, S. V.; Simic, M. G. *Biochim. Biophys. Acta* **1989**, *1008*, 39.
- (15) Cullis, P. M.; Jones, G. D. D.; Symons, M. C. R.; Lea, J. S. *Nature* **1987**, *330*, 773.
- (16) (a) Wagenknecht, H. A.; Stemp, E. D. A.; Barton, J. K. *J. Am. Chem. Soc.* **2000**, *122*, 1. (b) Wagenknecht, H. A.; Stemp, E. D. A.; Barton, J. K. *Biochemistry* **2000**, *39*, 5483.
- (17) (a) Koppenol, W. H.; Margoliash, E. *J. Biol. Chem.* **1982**, *257*, 4426. (b) Koppenol, W. H.; Rush, J. D.; Mills, J. D.; Margoliash, E. *Mol. Biol. Evol.* **1991**, *8*, 545.
- (18) (a) Green, D. R.; Reed, J. C. *Science* **1998**, *281*, 1309. (b) Yang, J.; Liu, X. S.; Bhalla, K. *Science* **1997**, *275*, 1129. (c) Kluck, R. M.; Bossy-Wetzel, E.; Green, D. R.; Newmeyer, D. D. *Science* **1997**, *275*, 1132.

- (19) Ramakrishnan, V. *Annu. Rev. Biophys. Biomol. Struct.* **1997**, *26*, 83.
- (20) Margoliash, E.; Frohwirt, N. *Biochem. J.* **1959**, *71*, 570.
- (21) Amouyal, E.; Homs, A.; Chambron, J.-C.; Sauvage, J.-P. *J. Chem. Soc., Dalton Trans.* **1990**, *6*, 1841.
- (22) (a) Yoshikawa, Y.; Yamasaki, K. *Coord. Chem. Rev.* **1979**, *28*, 205. (b) Dupureur, C.; Barton, J. K. *Inorg. Chem.* **1997**, *36*, 33.
- (23) Brautigan, D. L.; Ferguson-Miller, S.; Margoliash, E. *Methods Enzymol.* **1978**, *53*, 128.
- (24) Meyer, T. J.; Taube, H. *Inorg. Chem.* **1968**, *7*, 2369.
- (25) Hartshorn, R. M.; Barton, J. K. *J. Am. Chem. Soc.* **1992**, *114*, 5919.
- (26) Holmlin, R. E.; Stemp, E. D. A.; Barton, J. K. *J. Am. Chem. Soc.* **1996**, *118*, 5236.

$$I_0/I = 1 + K_{SV}[Q] \quad (1)$$

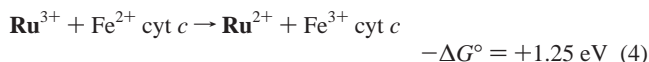
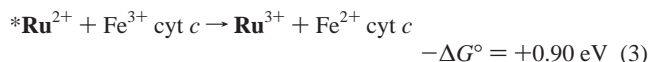
$$k_q = K_{SV}/\tau_{\text{avg}} \quad (2)$$

K_{SV} is the Stern–Volmer constant (obtained from plots of I_0/I vs $[Q]$), and τ_{avg} is the average emission lifetime in the absence of quencher. Plots of τ_0/τ were generated in an analogous manner, where τ_0 is the emission lifetime in the absence of quencher and τ is the emission lifetime at $[Q]$.

Absorbance Difference Spectra. Photoexcitation of DNA-bound $\text{Ru}(\text{phen})_2\text{dppz}^{2+}$ produces $^*\text{Ru}(\text{phen})_2\text{dppz}^{2+}$, which gives rise to a long-lived transient upon quenching with $\text{Ru}(\text{NH}_3)_6^{3+}$ or Fe^{3+} cyt *c*. To generate the absorbance difference spectra of kinetic transients, individual data traces from single wavelengths were fit to an exponential function at times $>5 \mu\text{s}$ and the absorbance changes were taken from the zero-time absorbances predicted by the fits. For the spectrum of the guanine radical generated by quenching $^*\text{Ru}(\text{phen})_2\text{dppz}^{2+}$ with $\text{Ru}(\text{NH}_3)_6^{3+}$ in poly(dG-dC), the data were taken from ref 8, where a similar procedure was used.

The Fe^{3+} – Fe^{2+} difference spectrum for cytochrome *c* was taken from ref 20. However, because others have observed perturbations in the cytochrome structure upon complexation with lipids²⁷ or anionic porphyrins,²⁸ we examined the absorbance spectra of Fe^{3+} cyt *c* and Fe^{2+} cyt *c* in the presence and absence of DNA under the experimental conditions used in this study. DNA had no effect on any of the individual spectra or upon the Fe^{3+} – Fe^{2+} difference spectrum. Within the resolution of our HP8453 UV–visible diode array spectrophotometer, the Fe^{3+} cyt *c* and Fe^{2+} cyt *c* spectra were not distinguishable from those reported by Margoliash and Frohwirt.²⁰ In transient absorption measurements, the 434 nm isosbestic point of the cytochrome was found manually by determining the wavelength of isoabsorbance for Fe^{3+} cyt *c* and Fe^{2+} cyt *c* solutions of equal concentration.

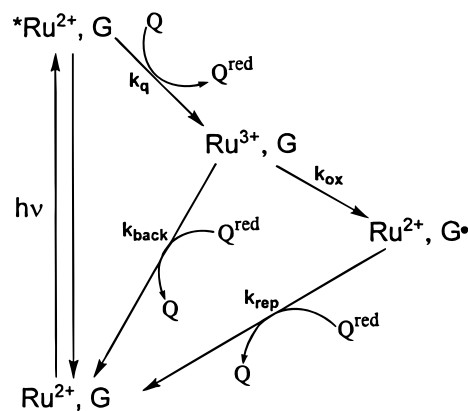
Reduction Potentials and Driving Forces for Electron-Transfer Reactions. All values are given versus NHE. $\text{Ru}(\text{phen})_2\text{dppz}^{2+}$, the photosensitive intercalator, has $E^\circ(\text{Ru}^{3+}/^*\text{Ru}^{2+}) = -0.65 \text{ V}$ and $E^\circ(\text{Ru}^{3+}/\text{Ru}^{2+}) = +1.6 \text{ V}$.²⁹ For the quenchers, $\text{Ru}(\text{NH}_3)_6^{3+}$ has $E^\circ(\text{Ru}^{3+}/\text{Ru}^{2+}) = +0.040 \text{ V}$ ²⁹ and cytochrome *c* has $E^\circ(\text{Fe}^{3+}/\text{Fe}^{2+}) = +0.25 \text{ V}$.³⁰ For the DNA bases, recently reported values include $E^\circ(\text{A}^+/\text{A}) = +1.4 \text{ V}$ for the adenine radical and $E^\circ(\text{G}^+/\text{G}) = +1.3 \text{ V}$ for the guanine radical;^{2c} the pyrimidine bases are considerably more difficult to oxidize. Electrochemical potentials of DNA bases are strongly dependent upon environmental conditions such as pH;^{2d} thus these values are only estimates for the potentials of DNA bases in double-stranded DNA polymers. Using these values and abbreviating $\text{Ru}(\text{phen})_2\text{dppz}$ as **Ru**, we depict the electron transfers under study as shown in eqs 3–6.



Results and Discussion

Description of the Flash–Quench Experiment. The flash–quench technique allows for the generation of the guanine radical in duplex DNA via 1-electron oxidation by intercalated $\text{Ru}(\text{phen})_2\text{dppz}^{3+}$. The reactions in this flash–quench experiment are summarized in Scheme 1. Visible excitation of the inter-

Scheme 1



calated donor (**Ru**²⁺) yields the excited-state donor (***Ru**²⁺), which can transfer an electron to a nonintercalating oxidative quencher (Q) to produce the oxidized donor (**Ru**³⁺) and the reduced quencher Q^{red}. At this point, **Ru**³⁺ thus formed can either undergo a back-electron-transfer reaction with Q^{red} or oxidize a nearby guanine (G) to generate the guanine radical, shown as G[•], because transient absorption measurements⁸ are consistent with rapid deprotonation to the neutral form.⁹ This guanine radical, in turn, can be reduced by Q^{red} to regenerate the system or can react further to give an irreversible oxidation product⁸ (not shown). Using the known differential absorption spectra of all the species involved in these reactions, it is possible to demonstrate electron transfer from Fe^{2+} cyt *c* to the guanine radical by transient absorption spectroscopy.

Difference Spectra Observed in Poly(dA-dT) and Poly(dG-dC) with Quenching of $\text{Ru}(\text{phen})_2\text{dppz}^{2+}$ by $\text{Ru}(\text{NH}_3)_6^{3+}$. When $^*\text{Ru}(\text{phen})_2\text{dppz}^{2+}$ intercalated in poly(dA-dT) is quenched by $\text{Ru}(\text{NH}_3)_6^{3+}$, a long-lived transient is observed, corresponding to the $\text{Ru}(\text{phen})_2\text{dppz}^{3+}/\text{Ru}(\text{NH}_3)_6^{2+}$ intermediate. Because the hexaammine complex has negligible absorbance above 300 nm ($\Delta\epsilon < 100 \text{ M}^{-1} \text{ cm}^{-1}$),²⁴ the observed spectrum (Figure 1) can be assigned solely to the Ru^{3+} – Ru^{2+} absorbance difference for the dppz complex. The spectrum is strongly negative in the 400–500 nm region, owing to the loss of the metal-to-ligand charge-transfer (MLCT) band that is characteristic of ruthenium polypyridyl complexes.³¹ It is interesting to note that, although oxidation of adenine by the $\text{Ru}(\text{III})$ metal–intercalator is thermodynamically possible, the dominant path for $\text{Ru}(\text{phen})_2\text{dppz}^{3+}$ reduction is the reaction with $\text{Ru}(\text{NH}_3)_6^{2+}$; no evidence for the adenine radical has been observed. Apparently, the lower driving force of the reaction of $\text{Ru}(\text{phen})_2\text{dppz}^{3+}$ with A does not allow base oxidation to compete effectively against the back-reaction with the reduced quencher.

In contrast, when $^*\text{Ru}(\text{phen})_2\text{dppz}^{2+}$ is quenched by $\text{Ru}(\text{NH}_3)_6^{3+}$ in the presence of poly(dG-dC), the resulting long-lived transient does not show the spectral characteristics of $\text{Ru}(\text{III})$. Instead, the spectrum observed for the long-lived transient⁸ (Figure 1) is indicative of the neutral guanine radical,⁹ being positive in the region 300–600 nm with broad maxima near 380 and 550 nm. The decay of the signal corresponds to the reaction between $\text{Ru}(\text{NH}_3)_6^{2+}$ and the guanine radical. Because the appearance of the guanine radical occurs concomitantly with the decay of $^*\text{Ru}(\text{phen})_2\text{dppz}^{2+}$, it is clear that the reaction of $\text{Ru}(\text{phen})_2\text{dppz}^{3+}$ with G is quite rapid and is limited

(27) (a) Spooner, P. J. R.; Watts, A. *Biochemistry* **1991**, *30*, 3871. (b) Hildebrandt, P.; Stockburger, M. *Biochemistry* **1989**, *28*, 6722. (c) Zhang, F.; Rowe, E. S. *Biochim. Biophys. Acta* **1994**, *1193*, 219. (28) Clark-Ferris, K. K.; Fisher, J. J. *Am. Chem. Soc.* **1985**, *107*, 5007. (29) (a) Murphy, C. J.; Arkin, M. R.; Ghatlia, N. D.; Bossmann, S.; Turro, N. J.; Barton, J. K. *Proc. Natl. Acad. Sci. U.S.A.* **1994**, *91*, 5315. (b) Arkin, M. R.; Kelley, S. O.; Hill, M. G. Unpublished results. (30) (a) Moore, G. R.; Pettigrew, G. W. *Cytochromes c*; Springer-Verlag: New York, 1990.

(31) (a) Kalyanasundaram, K. *Coord. Chem. Rev.* **1982**, *46*, 159. (b) Juris, A.; Balzani, V.; Barigelletti, F.; Campagna, S.; Balsler, P.; Von Zelewsky, A. *Coord. Chem. Rev.* **1988**, *84*, 85.

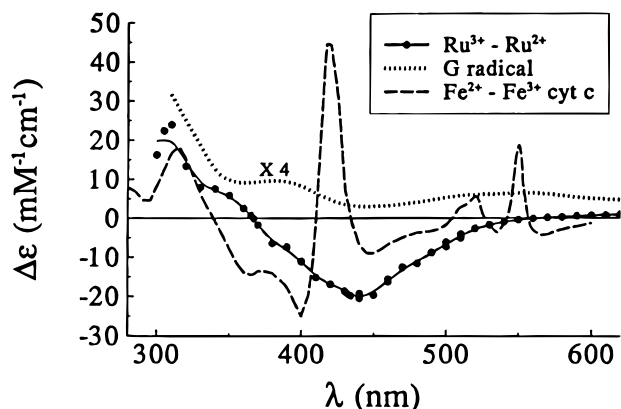


Figure 1. Absorbance difference spectra of species formed during the flash-quench experiment. Shown are the spectrum for the guanine radical (dotted line, adapted from ref 8), the $\text{Fe}^{2+}-\text{Fe}^{3+}$ difference spectrum for cytochrome *c* (dashed line, adapted from ref 20), and the $\text{Ru}^{3+}-\text{Ru}^{2+}$ difference spectrum for $\text{Ru}(\text{phen})_2\text{dppz}^{2+}$ bound to DNA. The $\text{Ru}^{3+}-\text{Ru}^{2+}$ difference spectrum was obtained by quenching $^*\text{Ru}(\text{phen})_2\text{dppz}^{2+}$ with $\text{Ru}(\text{NH}_3)_6^{3+}$ in the presence of poly(dA-dT); conditions were $20 \mu\text{M}$ $\text{Ru}(\text{phen})_2\text{dppz}^{2+}$, $200 \mu\text{M}$ $\text{Ru}(\text{NH}_3)_6^{3+}$, and 2 mM nucleotides in 5 mM NaPi, 50 mM NaCl (pH 7) at 20°C . The extinction coefficient of the guanine radical in duplex DNA is not known; this spectrum is based on an estimate of $\epsilon_{390} = 2.6 \text{ mM}^{-1} \text{ cm}^{-1}$ (from ref 9) and is multiplied by a factor of 4 for purposes of presentation.

by the quenching process. This means that $k_{\text{ox}} \gg k_{\text{q}}[\text{quencher}]$ (Scheme 1), with a lower limit of $2 \times 10^8 \text{ s}^{-1}$.⁸

Figure 1 also shows the $\text{Fe}^{2+}-\text{Fe}^{3+}$ difference spectrum for cytochrome *c*, as reported by Margoliash and Frohwirt.²⁰ Features of note in this spectrum include a maximum at 550 nm ($\Delta\epsilon = +19.6 \text{ mM}^{-1} \text{ cm}^{-1}$) and isosbestic points at 339, 410, 434, 504, 526, 542, and 556 nm.

Quenching of DNA-Bound $^*\text{Ru}(\text{phen})_2\text{dppz}^{2+}$ by Fe^{3+} cyt *c*. Electron transfer from excited-state $\text{Ru}(\text{phen})_2\text{dppz}^{2+}$ to Fe^{3+} cyt *c* is favorable by $\sim 0.90 \text{ V}$, and ferricytochrome *c* is indeed an efficient quencher of $^*\text{Ru}^{2+}$ emission in both poly(dA-dT) and poly(dG-dC). Figure 2A shows a Stern-Volmer plot of the steady-state emission quenching, with intensities obtained by integrating under the time-resolved luminescence decay curves. The quenching titrations give slightly upward-curving I_0/I plots and are nearly identical for the two DNAs.³²

Time-resolved luminescence measurements indicate that this quenching process is dynamic, i.e., occurring on the time scale of the excited-state decay. The intercalated ruthenium complex has different emission decay kinetics in the two polymers, as seen previously.³³ The emission in poly(dG-dC) is well-described by a monoexponential function with a lifetime (τ) of 230 ns,³⁴ whereas for poly(dA-dT), the luminescence decay is biexponential, with $\tau_1 = 120 \text{ ns}$ (84%) and $\tau_2 = 690 \text{ ns}$ (16%). Figure 2B (inset) shows the luminescence decay curves of $\text{Ru}(\text{phen})_2\text{dppz}^{2+}$ during a titration with Fe^{3+} cyt *c* in poly(dG-

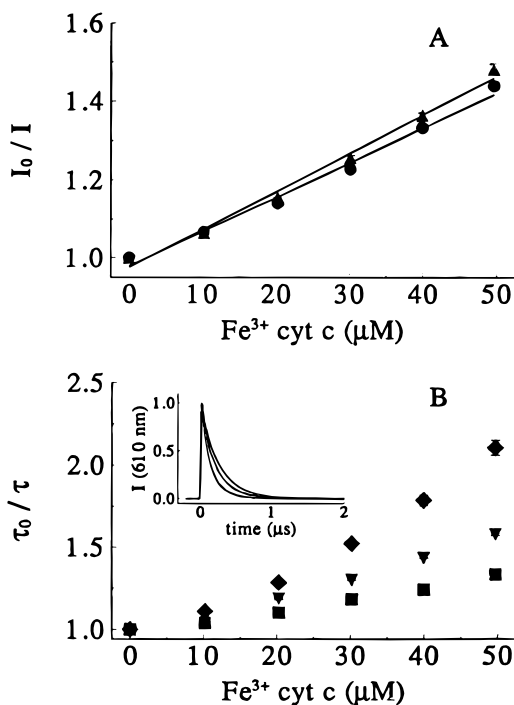


Figure 2. Steady-state (A) and lifetime (B) quenching of $^*\text{Ru}(\text{phen})_2\text{dppz}^{2+}$ titrated with Fe^{3+} cyt *c* in the presence of poly(dA-dT) or poly(dG-dC). (A) Shown are data for $^*\text{Ru}(\text{phen})_2\text{dppz}^{2+}$ bound to poly(dG-dC) (circles) and poly(dA-dT) (triangles). The data are plotted as I_0/I vs quencher concentration, where I is emission intensity and I_0 is emission intensity with no quencher. The lines represent linear fits to the data. (B) Shown are lifetime quenching data for $^*\text{Ru}(\text{phen})_2\text{dppz}^{2+}$ bound to poly(dG-dC) and poly(dA-dT) ($\tau_1 =$ squares, $\tau_2 =$ diamonds). Inset: Normalized 610 nm emission decay curves for $^*\text{Ru}(\text{phen})_2\text{dppz}^{2+}$ bound to poly(dG-dC), in the presence of 0, 20, and $50 \mu\text{M}$ Fe^{3+} cyt *c*. Conditions: $10 \mu\text{M}$ $\text{Ru}(\text{phen})_2\text{dppz}^{2+}$; 1 mM nucleotides in a buffer of 5 mM tris, 5 mM NaCl (pH 8) at 20°C .

dC). As the concentration of cytochrome *c* increases, the emission lifetime decreases, consistent with dynamic quenching. That the quenching is dynamic is also evident from the fact that I_0/I and τ_0/τ increase by the same amount, both reaching a value of ~ 1.5 by the end of the titration (Figure 2B). For the AT polymer, the quenching is also dynamic, although a differential quenching of the two emission lifetimes makes a direct correlation between I_0/I and τ_0/τ less obvious; with poly(dA-dT), the shorter component (τ_1) is quenched less efficiently than the longer component (τ_2).

The intensity quenching data were used to estimate quenching constants for ferricytochrome *c* in the two polymers. Linear fits to the I_0/I plots give Stern-Volmer constants (K_{SV}), here yielding $K_{\text{SV}}(\text{AT}) = 1.1 \times 10^4 \text{ M}^{-1}$ for the AT polymer and $K_{\text{SV}}(\text{GC}) = 9.7 \times 10^3 \text{ M}^{-1}$ for the GC polymer. Upon conversion of the Stern-Volmer constants to quenching constants (k_{q}) based upon the weight-averaged emission lifetimes, one obtains $k_{\text{q}}(\text{AT}) = 5.2 \times 10^{10} \text{ M}^{-1} \text{ s}^{-1}$ and $k_{\text{q}}(\text{GC}) = 4.2 \times 10^{10} \text{ M}^{-1} \text{ s}^{-1}$ (Table 1). These values indicate efficient quenching of the DNA-bound intercalator by Fe^{3+} cyt *c*. However, they do not indicate that the quenching occurs faster than diffusion. In earlier studies where ruthenium polypyridyl complexes bound to DNA were quenched by cationic complexes, the DNA accelerated the reaction because the reactants concentrated in the electrostatic field of the DNA.³⁵ A similar effect surely applies here as well. Nonetheless, it should be noted that

(32) With $\text{Ru}(\text{NH}_3)_6^{3+}$ as surface-bound quencher, contrasting Fe^{3+} cyt *c*, we observed a strong difference in quenching between the polymers, which we attributed to differences in access to the DNA-bound metallointercalator.^{33a} It is likely that smaller quenchers can more intimately distinguish the different binding geometries of the metallointercalator in these polymers than can the cytochrome.

(33) (a) Stemp, E. D. A.; Holmlin, R. E.; Barton, J. K. *Inorg. Chim. Acta* **2000**, *297*, 88. (b) Jenkins, Y.; Friedman, A. E.; Turro, N.; Barton, J. K. *Biochemistry* **1992**, *31*, 10809–10816. (c) Tuite, E.; Lincoln, P.; Norden, B. *J. Am. Chem. Soc.* **1997**, *119*, 239.

(34) Although we and others have observed a biexponential decay for the emission of $\Delta\text{-Ru}(\text{phen})_2\text{dppz}^{2+}$ bound to poly(dG-dC),³³ a monoexponential function was sufficient to describe the emission under these conditions.

(35) Orellana, G.; Kirsch-De Mesmaeker, A.; Barton, J. K.; Turro, N. J. *Photochem. Photobiol.* **1991**, *54*, 499.

Table 1. Kinetic Constants for Electron-Transfer Reactions with Cytochrome *c*

| DNA | Fe ³⁺ → Fe ²⁺ | | Fe ²⁺ → Fe ³⁺ |
|-------------|--|--|--|
| | K_{SV} (10 ⁴ M ⁻¹) ^a | k_q (10 ¹⁰ M ⁻¹ s ⁻¹) ^b | k_2 (10 ¹⁰ M ⁻¹ s ⁻¹) ^c |
| poly(dA-dT) | 1.1 | 5.2 | 28 |
| poly(dG-dC) | 0.97 | 4.2 | 2.0 |

^a Stern–Volmer constants were obtained from linear fits to the I_0/I data (Figure 2A). ^b Quenching constants were calculated from $k_q = K_{SV}/\tau_{avg}$, where τ_{avg} is the average weighted lifetime of the luminescence; $\tau_{avg} = 232$ ns for poly(dG-dC) and 211 ns for poly(dA-dT). ^c Biomolecular rate constants (k_2) for ferrocyanide oxidation were obtained from slopes in plots of $1/\Delta A(550 \text{ nm})$ vs time (Figure 5).

bimolecular constants of $\sim 10^{10} \text{ M}^{-1} \text{ s}^{-1}$ are possible for two large reactants of opposite charge,³⁶ i.e., the positively charged cytochrome and the negatively charged DNA holding the intercalator.

It is reasonable to assign the primary quenching mechanism as electron transfer, given (i) the high driving force for the reaction, (ii) the observation of redox quenching in ruthenated cytochromes *c*,^{10,11,37} and (iii) our detection of the electron-transfer products (vide infra). However, some fraction of energy-transfer quenching probably occurs, given the overlap between the Ru(phen)₂dppz²⁺ emission and the 695 nm charge-transfer band of ferrocyanide. Such energy transfer has been proposed to occur in ruthenated cytochrome *c*³⁸ and was recently demonstrated for Ru(bpy)₃-labeled substrates bound to cytochrome P450.³⁹

Difference Spectra Observed in Poly(dA-dT) and Poly(dG-dC) with *Ru(phen)₂dppz²⁺ Quenched by Fe³⁺ cyt *c*. The quenching reaction we observe results in the formation of long-lived transient species, readily monitored by transient absorption spectroscopy, for which the spectral characteristics depend on the identity of the DNA polymer. In Scheme 1, if we consider Fe³⁺ cyt *c* as the oxidative quencher of Ru(phen)₂dppz²⁺, then an intermediate consisting of Ru(III) and Fe²⁺ cyt *c* would be formed. This intermediate would have two possible fates: (i) it could decay by direct back-reaction of Ru(III) with Fe²⁺ cyt *c*, or (ii) the Ru(III) intercalator could oxidize a nearby guanine to form the guanine radical, leaving [G•, Fe²⁺ cyt *c*] as the intermediate. For this latter intermediate, the resulting electron transfer from Fe²⁺ cyt *c* to G• is favored by ~ 1 V and would constitute repair of a hole on guanine by a redox-active protein.

It is useful to first consider the transients formed in the presence of poly(dA-dT). Figure 3A shows the long-lived transients at 550 and 434 nm formed by quenching *Ru(phen)₂dppz²⁺ with Fe³⁺ cyt *c*. The signal is positive at 550 nm, where the Fe²⁺–Fe³⁺ cyt *c* difference spectrum has a maximum due to absorption of the α band of the ferrocyanide. In contrast, the signal is negative at 434 nm, where the Fe²⁺–Fe³⁺ cyt *c* difference spectrum has an isosbestic point and where the Ru³⁺–Ru²⁺ difference spectrum is negative (Figure 1).

Upon comparison with Figure 1, it is apparent that the difference spectrum of the long-lived transient in poly(dA-dT) (Figure 4, circles) is essentially the sum of the Fe²⁺–Fe³⁺ cyt *c* difference spectrum and the Ru³⁺–Ru²⁺ spectrum. In particular,

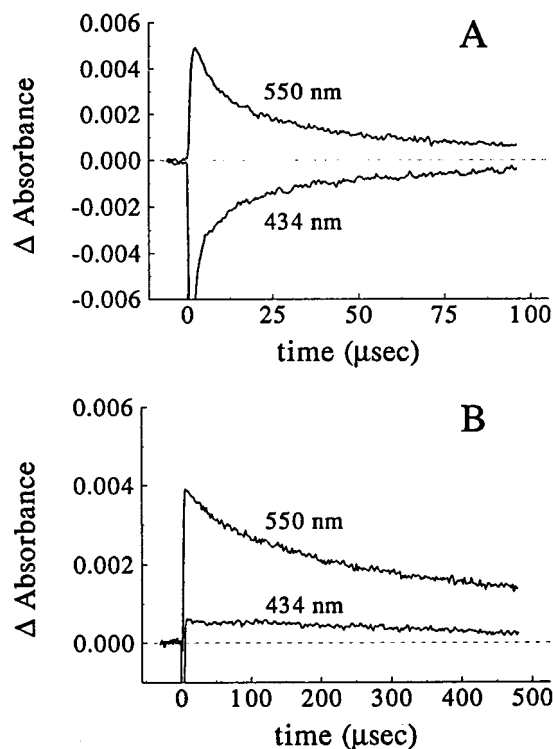


Figure 3. Long-lived transients at 550 and 434 nm formed upon quenching of *Ru(phen)₂dppz²⁺ by Fe³⁺ cyt *c* in the presence of poly(dA-dT) (A) and poly(dG-dC) (B). 550 nm represents a maximum in the Fe²⁺–Fe³⁺ difference spectrum of cyt *c*, while 434 nm is an isosbestic point; the former wavelength thus allows for detection of the oxidation state of the cyt *c*, while the latter wavelength permits the monitoring of the other species present, without interference from the cytochrome. The data traces at 434 nm have a large negative spike owing to the excited-state decay of *Ru(phen)₂dppz²⁺; the data were truncated to emphasize the portion of the signal that persists beyond the time scale of the excited state. Conditions: 20 μM Fe³⁺ cyt *c*; others as for Figure 2.

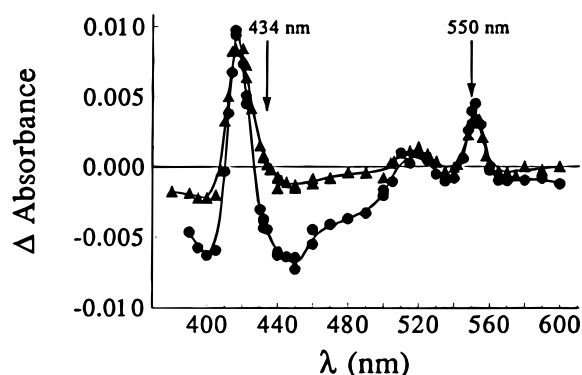


Figure 4. Absorbance difference spectra of long-lived transients formed upon quenching of *Ru(phen)₂dppz²⁺ by Fe³⁺ cyt *c* in the presence of poly(dA-dT) (circles) and poly(dG-dC) (triangles). To generate the transient absorption spectra, individual data traces from single wavelengths were fit to an exponential function at times $> 5 \mu\text{s}$ and the absorbance changes were then obtained from the zero-time absorbance predicted from the fit. The lines through the data points are simply visual guides. Conditions: 40 μM Fe³⁺ cyt *c*; others as for Figure 2.

the spectrum of the transient resembles that of cyt *c* in the region from 500 to 600 nm, where the absorbance changes owing to the ruthenium complex are small, whereas the spectrum of the transient from 430 to 500 nm is dominated by the negative ΔA in the spectrum of the ruthenium complex observed upon oxidation. This difference spectrum, coupled with the fact that the signals at 550 nm (Fe²⁺ cyt *c*) and 434 nm (Ru³⁺) are

- (36) Berg, O. G.; von Hippel, P. H. *Annu. Rev. Biophys. Biophys. Chem.* **1985**, *14*, 131.
 (37) Mines, G. A.; Bjerrum, M. J.; Hill, M. G.; Casimiro, D. R.; Chang, I.-J.; Winkler, J. R.; Gray, H. B. *J. Am. Chem. Soc.* **1996**, *118*, 1961.
 (38) Mines, G. Ph.D. Thesis, California Institute of Technology, 1997.
 (39) Dmochowski, I. J.; Crane, B. R.; Wilker, J. J.; Winkler, J. R.; Gray, H. B. *Proc. Natl. Acad. Sci. U.S.A.* **1999**, *96*, 12987.

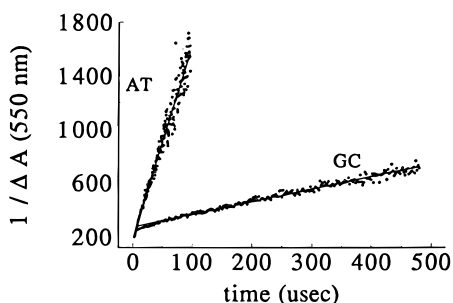


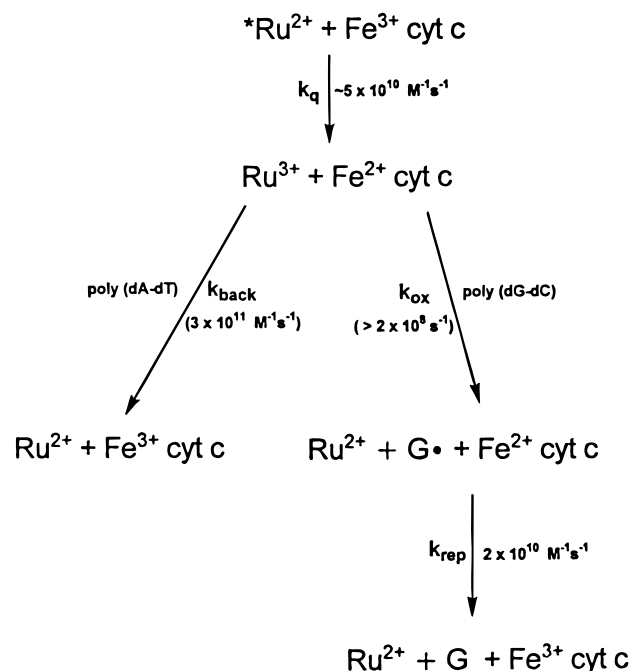
Figure 5. Kinetics of ferrocyclochrome *c* oxidations monitored at 550 nm. The decays of the 550 nm signals, representing the disappearance of Fe^{2+} cyt *c*, were plotted as inverse absorbance vs time to determine the orders of the reactions. To eliminate interference from the $^*\text{Ru}(\text{phen})_2\text{dppz}^{2+}$ excited state, the portions of the signals occurring before 3 μs were deleted from the data set. The slopes were converted to bimolecular rate constants (k_2) using $\Delta\epsilon_{550} = +19.6 \text{ mM}^{-1} \text{ cm}^{-1}$ for poly(dA-dT) and $\Delta\epsilon_{550} = +21 \text{ mM}^{-1} \text{ cm}^{-1}$ for poly(dG-dC); this gave $k_2 = 2.8 \times 10^{11} \text{ M}^{-1} \text{ s}^{-1}$ and $2.0 \times 10^{10} \text{ M}^{-1} \text{ s}^{-1}$ for the GC and AT polymers, respectively. Conditions: 40 μM Fe^{3+} cyt *c*; others as for Figure 2.

opposite in sign but exhibit the same kinetics, suggests that the oxidation of Fe^{2+} cyt *c* is synchronous with the reduction of $\text{Ru}(\text{phen})_2\text{dppz}^{3+}$, i.e., that the observed electron transfer is from Fe^{2+} cyt *c* to the oxidized metallointercalator. The fact that the metal complex directly oxidizes the ferrocyclochrome rather than adenine (A) is not surprising, given the expected low driving force for oxidation of A by $\text{Ru}(\text{phen})_2\text{dppz}^{3+}$ and that oxidation of A was not apparent when $^*\text{Ru}(\text{phen})_2\text{dppz}^{2+}$ was quenched by $\text{Ru}(\text{NH}_3)_6^{3+}$.

Different results are seen for the GC polymer. In this case, the individual signals at 550 and 434 nm are both positive (Figure 3B). If the transient species contained an Ru^{3+} – Ru^{2+} component, a negative signal would be observed at 434 nm (vide supra). The presence of a small positive signal is instead consistent with the presence of G^* as the other absorbing species. Since oxidation of G by $\text{Ru}(\text{phen})_2\text{dppz}^{3+}$ has already been shown to occur synchronously with the oxidation of $^*\text{Ru}(\text{phen})_2\text{dppz}^{2+}$ by $\text{Ru}(\text{NH}_3)_6^{3+}$ (in $\sim 50 \text{ ns}$),⁸ one would expect that oxidation of G by $\text{Ru}(\text{phen})_2\text{dppz}^{3+}$ might also occur quickly upon quenching of $^*\text{Ru}(\text{phen})_2\text{dppz}^{2+}$ by Fe^{3+} cyt *c*.⁴⁰

The difference spectrum of the intermediate supports this notion. The spectrum of the transient formed in poly(dG-dC) (Figure 4, triangles) is roughly the sum of the G^* –G and Fe^{2+} – Fe^{3+} cyt *c* difference spectra. The spectrum is understandably dominated by the cytochrome, since its absorptivity at most wavelengths is typically an order of magnitude larger than that of the guanine radical. Hence, it is not possible to obtain a full spectroscopic characterization of the guanine radical. Nonetheless, careful selection of the monitoring wavelength allows for the detection of the weak chromophore in the presence of the stronger chromophore. In this case, the absorbance signals were monitored at the Fe^{2+} – Fe^{3+} difference spectrum isosbestic points²⁰ in order to eliminate interference from the strongly absorbing cytochrome. Thus, the observation of positive signals at the Fe^{2+} – Fe^{3+} cyt *c* difference spectrum isosbestic points of 339, 410, 434, 504, 526, 542, and 556 nm indeed indicates

Scheme 2



that the guanine radical is the other absorbing species, since the G^* –G difference spectrum is positive throughout this wavelength range.⁸ Thus, upon the quenching of $^*\text{Ru}(\text{phen})_2\text{dppz}^{2+}$ by Fe^{3+} cyt *c* in poly(dG-dC), electron transfer from Fe^{2+} cyt *c* to the guanine radical is observed. This represents one of the few directly observable electron transfers, thus far, between DNA and a protein.

Kinetics of Ferrocyclochrome *c* Oxidation. With each DNA polymer, the oxidation of ferrocyclochrome *c* is a second-order process, as indicated by the linear plots of $1/\Delta A(550 \text{ nm})$ versus time (Figure 5). Extracting the bimolecular rate constants (k_2) from linear fits to the data, one obtains $k_2(\text{AT}) = 2.8 \times 10^{11} \text{ M}^{-1} \text{ s}^{-1}$ and $k_2(\text{GC}) = 2.0 \times 10^{10} \text{ M}^{-1} \text{ s}^{-1}$, the latter value giving the kinetics of the reaction between the guanine radical and ferrocyclochrome *c*. As for the quenching reactions, the large magnitudes of their rate constants reflect not that the reactions are faster than diffusion but rather the reduction in dimensionality associated with the concentration of reactants in the electrostatic field of the DNA polymer.³⁵ Nonetheless, even with micromolar concentrations of protein, this bimolecular chemistry occurs for the most part in less than 1 ms, suggesting that such reactions, even between nonphysiological partners, could compete *in vivo* with formation of DNA lesions such as 8-oxoguanine.⁴¹

Whereas the quenchings of intercalated $\text{Ru}(\text{phen})_2\text{dppz}^{2+}$ by Fe^{3+} cyt *c* are very similar for poly(dG-dC) and poly(dA-dT), the kinetics for ferrocyclochrome *c* oxidation vary by 1 order of magnitude. This 10-fold difference in rate may result from the fact that there are different partners for reaction with cytochrome *c* in the two polymers: the protein reacts with the intercalated metal complex in poly(dA-dT) and with the guanine radical in poly(dG-dC). It is reasonable to consider that closer contact between the ferrocyclochrome and its oxidant might be more

(40) The amplitudes of the long-lived portion of the 550 nm signal and of the short-lived negative spike in the 434 nm signal can be used to obtain approximate concentrations of Fe^{2+} cyt *c* and $^*\text{Ru}(\text{phen})_2\text{dppz}^{2+}$, respectively. From these concentrations and the observed quenching, we estimate that $>40\%$ of the quenched $^*\text{Ru}(\text{phen})_2\text{dppz}^{2+}$ produces a long-lived Fe^{2+} cyt *c* transient and thus a guanine radical; the remaining 60% either undergoes a fast back electron transfer or is quenched by another mechanism.

(41) Transient absorption measurements suggest that the guanine radical in duplex DNA can persist for hundreds of milliseconds, a result also consistent with EPR detection of the guanine radical (Schiemann, O.; Turro, N. J.; Barton, J. K. Submitted for publication). It is interesting that reaction of the guanine radical with micromolar concentrations of protein appears to be faster than reaction with H_2O and O_2 to form irreversibly oxidized products such as 8-oxoguanine.

facile for the bulky, solvent-exposed metal complex than for the guanine radical.

A summary of these results is given in Scheme 2 and Table 1. Quenching of $^*\text{Ru}^{2+}$ by Fe^{3+} cyt *c* is fast and occurs with similar efficiencies in both poly(dA-dT) and poly(dG-dC), with $k_q \sim (4-5) \times 10^{10} \text{ M}^{-1} \text{ s}^{-1}$. In the case of poly(dA-dT), Ru^{3+} then oxidizes Fe^{2+} cyt *c* to regenerate the resting state, with $k_{\text{back}} = 3 \times 10^{11} \text{ M}^{-1} \text{ s}^{-1}$. However, with poly(dG-dC), the back-reaction between oxidized metallointercalator and ferrocycytochrome *c* is not observed. Instead, Ru^{3+} rapidly oxidizes G with a rate constant k_{ox} , which has a lower limit of $2 \times 10^8 \text{ s}^{-1}$.⁸ The guanine radical is then repaired by electron transfer from Fe^{2+} cyt *c*, with rate constant $k_{\text{rep}} = 2 \times 10^{10} \text{ M}^{-1} \text{ s}^{-1}$.

It is perhaps surprising that there is any reaction at all between ferrocycytochrome *c* and the guanine radical. The guanine base is located in the interior base stack of the DNA, while the ferroheme of cyt *c* is mostly protected from solvent,^{30,42} with the metal center several angstroms from the protein surface. Clearly, these conditions are not optimal for close contact between donor and acceptor. Perhaps the mobility of the guanine radical in double-stranded DNA¹⁰ helps to facilitate reaction with the cytochrome, eliminating the necessity for the protein to search the entire DNA surface for its redox partner.

Implications for DNA Repair. Using cytochrome *c* as the oxidative quencher of a DNA-bound metallointercalator, an electron hole created on a guanine base was therefore shown to be filled by protein. While interactions between cyt *c* and DNA may not have direct physiological relevance, this experimental approach could be extended to any protein that has a redox-active group near the protein surface to undergo electron transfer

with the DNA. Besides hemes, redox-active groups capable of reducing the guanine radical include the easily oxidizable side chains of tyrosine and tryptophan.⁴³ Using the flash-quench method to study interactions of Lys-Trp-Lys with the guanine radical, we recently found that intercalated tryptophan reduces the guanine radical quite efficiently.¹⁶ One could imagine such aromatic residues in proteins bound to DNA functioning as relays, transferring oxidative damage from DNA to a redox cofactor. This notion is particularly intriguing, given that there are several DNA-binding proteins that contain FeS clusters.⁴⁴⁻⁴⁶ Whether such proteins can function in part to repair guanine radicals in vivo needs now to be determined.

Acknowledgment. We are grateful for grants from the NIH (GM 49216 to J.K.B.), the NSF (MCB981-7338 to E.D.A.S.), and Mount St. Mary's College Professional Development Fund (to E.D.A.S.) for financial support of this work. We also thank Prof. E. Margoliash, Dr. J. Rack, and Dr. I. Dmochowski for helpful discussions and Dr. O. Schiemann, Dr. H.-A. Wagenknecht, and C. Treadway for carefully reading the original manuscript.

IC0000698

(42) Bushnell, G. W.; Louie, G. V.; Brayer, G. D. *J. Mol. Biol.* **1990**, *214*, 585.

- (43) (a) Kim, S. T.; Heelis, P. F.; Sancar, A. *Redox-Act. Amino Acids Biol.* **1995**, *258*, 319. (b) Jovanovic, S. V.; Harriman, A.; Simic, M. G. *J. Phys. Chem.* **1986**, *90*, 1935. (c) DeFillipis, M. R.; Murthy, C. P.; Broitman, F.; Weinraub, D.; Faraggi, M.; Klapper, M. H. *J. Phys. Chem.* **1991**, *95*, 3416.
- (44) (a) Cunningham, R. P.; Asahara, H.; Bank, J. F.; Scholes, C. P.; Salerno, J. C.; Surerus, K.; Munck, E. *Biochemistry* **1989**, *28*, 4450. (b) Fu, W.; O'Handley, S.; Cunningham, R. P.; Johnson, M. K. *J. Biol. Chem.* **1992**, *267*, 16135.
- (45) Porello, S. L.; Cannon, M. J.; David, S. S. *Biochemistry* **1998**, *37*, 6465.
- (46) Uden, G.; Trageser, M.; Duchene, A. *Mol. Microbiol.* **1990**, *4*, 315.